Int J Earth Sci (Geol Rundsch) (2007) 96:1163–1178
DOI 10.1007/s00531-006-0149-8

ORIGINAL PAPER

A paleomagnetic study of the Basque Arc (Basque-Cantabrian Basin, Western Pyrenees)

M. Calvo-Rathert · J. Cuevas · J. M. Tubía · M. F. Bógalo · A. Gogichaishvili

Received: 25 April 2006 / Accepted: 23 November 2006 / Published online: 19 January 2007
© Springer-Verlag 2007

Abstract The Basque Arc constitutes the northern segment of the Basque-Cantabrian basin, in the western part of the Pyrenees. The main goal of the present study was to find out by means of paleomagnetic analysis if the arched shape of the Basque Arc has a primary origin, due to the development of sedimentary basins related to the opening of the Bay of Biscay or a secondary origin due to rotations about vertical axes. Nine volcanic flows of late Albian to Santonian age (100–83.5 My) were sampled together with 10 sedimentary sites (marls, limestones, calcarenites and sandstones) of lower Jurassic to early Eocene age in order to carry out paleomagnetic and rock-magnetic experiments, 15 paleodirections being obtained. In order to analyse these results together with data from previous studies, the studied area was subdivided into a western, a central and an eastern sector. While inclinations of all three sectors show a similar value, declinations differ. The western sector displays a 37 ± 16° clockwise rotation of its mean paleodeclination, the central sector is not rotated (4 ± 9°) and both sedimentary sites which make up the eastern sector show counter-clockwise rotations (–25 ± 11° and –68 ± 9°). These results suggest that the shape of the Basque Arc does not have a primary origin, but a secondary origin due to rotations about vertical axes as a result of differential shortening related to post-Lutetian compressive tectonics which resulted in the formation of the Pyrenees.

Keywords Paleomagnetism · Tectonics · Iberia · Basque-Cantabrian basin · Western Pyrenees · Rotations

M. Calvo-Rathert (✉) · M. F. Bógalo
Dpto. Física, Escuela Politécnica Superior,
Universidad de Burgos, Av. Cantabria, s/n,
09006 Burgos, Spain
e-mail: mcalvo@ubu.es

J. Cuevas · J. M. Tubía
Dpto. Geodinámica, Fac. Ciencias,
Universidad del País Vasco, Aptdo. 644,
48080 Bilbao, Spain

A. Gogichaishvili
Instituto de Geofísica,
Universidad Nacional Autónoma de México,
Ciudad Universitaria, Mexico City, Mexico

Introduction

The Basque Arc (Feuillée and Rat 1971) constitutes the northern segment of the Basque-Cantabrian basin, which is located in the western part of the Pyrenees (Fig. 1), a crustal domain shortened during late Cretaceous–Eocene Alpine orogeny between the Iberian and European Plates. Structural analysis of the Basque Arc shows that it is an example of positive inversion tectonics, with great geometric complexity, probably due to three superimposed geological processes. The first one corresponds to the generation of isolated strike-slip basins of small size, related to the left-lateral displacement of the Iberian Plate relative to the European Plate during Lower Cretaceous (Olivet 1996). The second one is related to the development of local basins, associated to widespread diapirism in the Basque Cantabrian basin, with halokinetic activity from Lower Cretaceous to Quaternary (Ríos 1948; Brinkmann and Lögters 1968). The third one can be ascribed to the regional compression of post-Lutetian (49 My) times due to the Pyrenean orogeny that

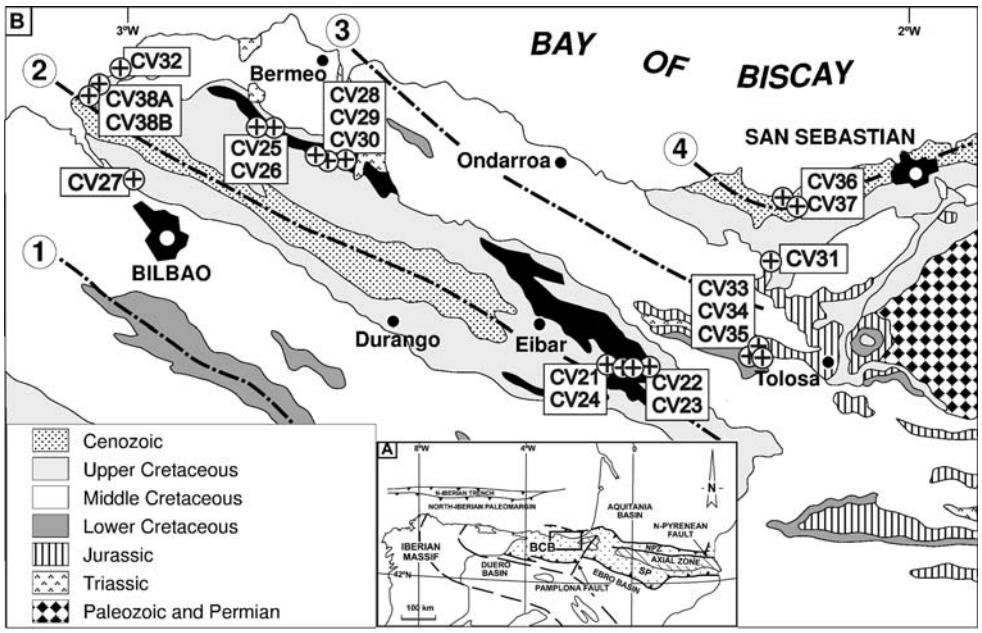


Fig. 1 Schematic map of the studied area. *A* Schematic map of the Pyrenean zone (modified from Cuevas and Tubía 1999). *BCB* Basque-Cantabrian basin; *NPF* North Pyrenean Fault; *NPZ* North Pyrenean Zone; *SPZ* South Pyrenean Zone; *PF* Pamplona fault. *Inset* shows the location of the Basque Arc in the Basque-Cantabrian basin. *B* Schematic geological map of the Basque Arc with location of sampled sites. *Black* Basic volcanic and subvolcanic rocks interlayered in the Upper Cretaceous of the Biscay Synclinorium. Trajectories of axial planes of the main cartographic folds in the Basque Arc: *1* Bilbao Anticlinorium; *2* Biscay Synclinorium; *3* North Bilbao Anticlinorium; *4* Guipuzcoa Monocline

replaced the subsidence regime that predominated in Mesozoic to Paleogene times. The reactivation of former syn-sedimentary normal faults as thrusts played a predominant role during the Tertiary evolution of the Basque Arc (Cuevas et al. 1999). As paleomagnetic data are a useful tool to study tectonic deformation by analysing the deflection of paleomagnetic directions, the main goal of the present study was to obtain information about possible vertical axis rotations in this area. These kind of data may allow to find out if the arched shape of the Basque Arc has a primary origin, due to the development of sedimentary basins related to the opening of the Bay of Biscay or a secondary origin due to rotations about vertical axes.

One of the main structures of the Pyrenees is the North Pyrenean Fault (NPF), a subvertical discontinuity that separates the Axial Zone to the south from the North Pyrenean Zone (NPZ) in the north (Choukroune 1976). In the Basque-Cantabrian Basin, however, the sedimentary rocks of the North-Pyrenean and South-Pyrenean zones come into contact because the Axial Zone is not represented there (Fig. 1). Highly conjectural and contradictory solutions have been proposed for the prolongation of the NPF through the Basque-Cantabrian basin (Boillot et al. 1973; Roest and Srivastava 1991; EVE 1995; Lefort and Agarwal 1999). The problem of locating the boundary between the NPZ and the SPZ is a major question, as they are interpreted to have belonged in Cretaceous times to the European and the Iberian plates respectively (e.g. Mattauer 1968; Choukroune et al. 1973).

The opening of the Bay of Biscay and the counter-clockwise rotation of the Iberian Plate relative to the Eurasian Plate are major features of Iberian tectonic history during Cretaceous. The rotation of Iberia is documented by paleomagnetic data and the interpretation of oceanic magnetic anomalies together with the plate tectonic reconstruction of the Bay of Biscay, but amount and timing of rotation are not fully established yet. Cretaceous paleomagnetic data from Iberia are scarce, but the amount of its counter-clockwise rotation has been inferred to be of the order of 35° (van der Voo 1993; Juárez et al. 1998). Analysis of oceanic magnetic anomalies suggests that the Bay of Biscay started to open at about the time of reversed polarity chron M0 (Srivastava et al. 1990; Malod and Mauffret 1990). Paleomagnetic results seem to frame the counter-clockwise rotation of Iberia between approximately 120 My (Aptian) and 85 My (Santonian) (e.g. Juárez et al. 1998).

As a result of the opening of the Bay of Biscay, a transcurrent motion of several hundred kilometres took place along the NPF (e.g. Olivet 1996), creating an extension zone in the Pyrenean domain. This

extensional domain appears in the NPZ and makes up a favourable setting for the genesis and emplacement of magmas of alkaline affinity (Azambre and Rossy 1976; Choukroune and Mattauer 1978), which could be sampled for the present study.

Although the area has traditionally been subject of magnetostratigraphic research, mainly due to the outcrop of well-exposed K/T sections (Roggenthen 1976; Mary et al. 1991; Moreau et al. 1994; Pujalte et al. 1995; Dinarès-Turell et al. 2002, 2003), paleomagnetic data obtained in the Basque Arc for tectonic purposes are very scarce (Vandenberg 1980), although some studies were carried out on units located in adjacent areas in the West (Stauffer and Tarling 1971; Schott and Peres 1987) and in the East (Larrasoaña et al. 2003a, b).

Geological setting and sampling

The Basque Arc is composed of sedimentary rocks of Triassic to Cenozoic age, which are folded facing northward. It is characterised by the existence of large folds, with axial traces running over more than 80 km. The main ones are the following (from south to north, Fig. 1): Bilbao Anticlinorium, Biscay Synclinorium, North Bilbao Anticlinorium and Guipuzcoa Monocline. These main structures display an arched shape, varying from a NW–SE azimuth near Bilbao at the west to a NE–SW trend west of Cinco Villas Massif. Inter-layered in the uppermost lower Cretaceous and Upper Cretaceous sedimentary rocks of the Biscay Synclinorium, the largest outcrops of basic alkaline rocks in the Pyrenees can be found.

Until the 1980s, geological studies on the Basque Arc considered the sedimentary rocks to be autochthonous. However, detailed structural studies and new available seismic and drilling data confirm the existence of important horizontal northward displacements, involving not only the Mesozoic and Tertiary cover but even the pre-Triassic basement (Cuevas et al. 1999; Gómez et al. 2002; Pedreira et al. 2003).

The Biscay Synclinorium (Fig. 1) is a late, composed NE-verging synform, that strikes N125°E, with an axis plunging smoothly (~10°) to NW. A subvertical foliation develops locally that strikes N120°E and is even found in the Tertiary Flysch of Middle Eocene age (Lutetian), deforming previous folds and thrusts. In its northern limb, chevron folds superimposed on previous folds with horizontal N130°E axes and verging to NE (Cuevas et al. 1982) can be found. These folds are associated to high-angle reverse faults that cut off the reverse limbs. The Southern limb of the Biscay Synclinorium is almost vertical.

In the Biscay Sinclinorium, stratigraphic order is preserved, and it can be seen that the older rocks, black shales and sandstones belonging to the so-called Supraurgonian Complex (''Black Flysch'' or ''North-Pyrenean Flysch'') of Albian age are mainly covered by carbonatic flysch sequences from Cenomanian to Coniacian ages.

A distinctive feature of the Biscay Synclinorium is a large outcrop of volcanic and subvolcanic rocks of basic composition (alkaline submarine basalts, dikes and picrite-teschenite sills) and vulcanodetritic rocks (cinerites and pillow-breccias) referred to as *Volcanic Complex* (Cuevas 1979; Mathey 1987; EVE 1995). It is worth noting that most of these magmatic rocks contain low-temperature mineral assemblages with albite, chlorite, prehnite and pumpellyite, blurring out partly or entirely the original magmatic phases, due to variable degrees of spilitization. These low-temperature mineral assemblages were probably formed at less than 200°C (Azambre and Rossy 1976). This alkaline magmatism can be only found along the North Pyrenean Zone, and its greatest thickness appears in the Biscay Synclinorium (Azambre and Rossy 1976; Cabanis and Le Furt-Balouet 1990). The volcanic complex is inter-layered with rocks from the Albian *Black Flysch* or North-Pyrenean Flysch to the Cenomanian *Calcareous Flysch* (Mathey 1987). According to micropaleontological data, volcanic activity took place from Upper Albian to Turonian, (105–89 My) (Lamolda et al. 1983). Geochronological data (K/Ar and $^{39}Ar/^{40}Ar$) from intrusive rocks (Montigny et al. 1986) allow distinguishing between two alkaline magmatic events in the Basque Country, an older one with an age comprised between 110 and 100 Ma, and a younger magmatic event of greater extension, with an age between 90 and 85 Ma. Some transformations in the pristine mineralogy of the alkaline basaltic rocks such as the chloritisation of pyroxenes could be related to the Cretaceous Pyrenean metamorphism between 95 and 85 Ma (Montigny et al. 1986; Golberg and Leyreloup 1990).

In the present study, we have taken samples from both volcanic and sedimentary sites (Fig. 1). The former consist of submarine volcanic rocks inter-layered in both limbs of the Biscay Sinclinorium. The sampled volcanic rocks belonged to submarine lava flows (pillow-lavas, pillow breccias and pyroclastics) of basaltic (plagioclase ± augite) to trachytic rocks (alkaline feldspar ± amphibole) of mainly late Albian (approximately 100 My) and Cenomanian (93.5–99.0 My) age (sites CV23, CV25, CV26, CV27, CV 28 and CV29). Three sites (CV21, CV22 and CV24) had a somewhat younger Coniacian to Santonian (83.5–89.0 My) age. Bedding correction data for volcanic sites, which were

characterised by steep dips (40–95°), were obtained from overlying and inter-layered sedimentary strata.

The sampled sedimentary sites were characterised by different ages and lithologies [CV30: Cenomanian marls; CV31: upper Cretaceous marly limestones; CV32: upper Cretaceous calcarenites; CV33: Oxfordian (154–159 My) marls and limestones; CV34: Pliensbachian (190–195 My) marls and limestones; CV35: Neocomian (121–144 My) marls and limestones; CV36: Ypresian (49.0–54.8 My) sandstones; CV37, CV38A and CV38B: Upper Paleocene (55.8–58.7 My) limestones, marls and calcarenites]. The thickness of the sampled sections of the sedimentary sites varied between approximately 2 and 10 m. Samples from sites CV38A and CV38B are respectively located on both limbs of the same fold, but besides these sites, only in site CV33 different bedding corrections had to be applied to different groups of samples. This prevented the use of the fold test in all other cases. A total of 7–14 samples (cores) were taken in each volcanic or sedimentary site and all samples were taken using a gasoline powered portable drill and oriented by means of a magnetic compass, as remanence of the small volcanic units (their intensity is discussed below) did not produce significant deflections of the compass needle during orientation.

Laboratory measurements and rock-magnetic results

Paleomagnetic experiments

Three or four pilot samples were taken for stepwise thermal demagnetisation in each of the 18 sites. Demagnetisation temperature in these preliminary experiments was increased in 35–65°C steps after performing an initial demagnetisation at a temperature between 98 and 130°C. Thermal cleaning was continued up to peak temperatures between 560 and 622°C. During thermal demagnetisation, susceptibility values at room temperature were measured after each heating step. In all sites except CV29, CV30 and CV38B at least one sample was also selected for stepwise alternating field cleaning in 1–30 mT steps up to peak field values of 110–60 mT. According to the results of these preliminary experiments, most volcanic samples were subjected to thermal demagnetisation, as in many cases demagnetisation plots provided by alternating field cleaning were less clear than those obtained by thermal treatment. In volcanic sites CV27 and CV28, however, both demagnetisation techniques were employed. In many sedimentary samples, a combination of both thermal and alternating field demagnetisation on the same samples provided better demagnetisation results. The samples of site CV30, however, were only thermally demagnetised.

Most paleomagnetic measurements were carried out in the paleomagnetic laboratory of the University of Burgos (Spain), but some were performed in the paleomagnetic laboratory of the Universidad Nacional Autónoma de México. Remanent magnetisation was measured either with a JR5A spinner magnetometer or a 2G cryogenic magnetometer. Thermal demagnetisation was performed with a Schonstedt TSD-1 furnace and AF-demagnetisation with a LDA-3A (Agico) demagnetiser, a degausser included in the 2G cryogenic magnetometer equipment (both in Burgos) as well as with a home made device (Mexico). Directions of remanent magnetisation components were determined in all cases by means of principal component analysis (Kirschvink 1980).

Rock-magnetic experiments

In order to identify minerals responsible for remanent magnetisation, susceptibility-versus-temperature (k–T) curves were measured in some representative samples from all sites, mainly with a KLY-2 Kappabridge and also with a Bartington susceptibility-meter with furnace. Whole rock powdered samples were heated up to temperatures near 700°C and cooled down to room temperature. Measurements were performed either in argon atmosphere or in vacuum. Curie points were determined taking inflexion points in k–T curves following the drop of susceptibility corresponding to the destruction of ferromagnetic phases. In several cases, k–T curves were measured for two samples belonging to the same site. As Curie-points from samples of the same site happened to be very similar, in Table 1 their mean value is shown.

Low-Ti titanomagnetite is the main (and often only) ferromagnetic phase observed (Fig. 2a; Table 1) in most volcanic samples. However, in CV29, besides low-Ti titanomagnetite, the presence of hematite (T_C = 660°C) could also be detected (Fig. 2b). In CV25, together with low-Ti titanomagnetite, another phase with a Curie temperature about 300°C was observed (Fig. 2c). A different behaviour can also be recognised in site CV23, in which the main ferromagnetic phase is pyrrothite together with magnetite (Fig. 2d). k–T curves could be measured only in some sedimentary sites (Table 1), as their susceptibility was characterised by weak values, of the order of 5×10^{-6} (SI-units) before the appearance of Hopkinson-peaks related to the presence of magnetite at temperatures above 400°C. All k–T curves measured on sedimentary

Table 1 Rock-magnetic results

Site	J_{NRM} ($Am^2Kg^{-1} \times 10^{-7}$)	T_C (°C)	AMS (P)	SIRM ($Am^2Kg^{-1} \times 10^{-4}$)	MDF (mT)	M_{RS}/M_S	H_{CR}/H_C
CV21 (V)	9,700 ± 200	582	1.069	2,443.3	65–70	0.158	1.54
CV22 (V)	4,600 ± 700	579	1.052		30–35	0.102	1.94
CV23 (V)	1,300 ± 200	337	1.050	54.4		0.059	
CV24 (V)	500 ± 120	588	1.026	197.6	35–40	0.360	1.62
CV25 (V)	110 ± 40	530	1.011	468.5		0.097	1.99
CV26 (V)	1,300 ± 60	557	1.025	1,168.6	15–20	0.158	1.76
CV27 (V)	13,000 ± 3,000	572	1.044	3,661.0	10–20	0.121	1.68
CV28 (V)	2,200 ± 400	575					
CV29 (V)	133 ± 18	552					
CV30 (S)	52 ± 3						
CV31 (S)	3.8 ± 0.3						
CV32 (S)	0.35 ± 0.03						
CV33 (S)	3.6 ± 0.5	616					
CV34 (S)	3.4 ± 0.9						
CV35 (S)	2.3 ± 0.6	574 (340)					
CV36 (S)	1.5 ± 0.2	568					
CV37 (S)	0.097 ± 0.006	581 (324)					
CV38A (S)	0.41 ± 0.06						
CV38B (S)	0.39 ± 0.10	587					

Site: *V* volcanic, *S* sedimentary site; J_{NRM}: mean NRM intensity in $Am^2Kg^{-1} \times 10^{-7}$; T_C: Curie temperature of the main ferromagnetic phase, Curie temperature of a minor pyrrothite fraction in sites CV35 and CV37 is also shown; AMS (P): anisotropy factor; SIRM: saturation isothermal remanence in $Am^2Kg^{-1} \times 10^{-4}$; MDF: median destructive field in mT; M_{RS}/M_S: saturation remanence to saturation magnetisation ratio; H_{CR}/H_C: remanent coercivity to coercivity ratio

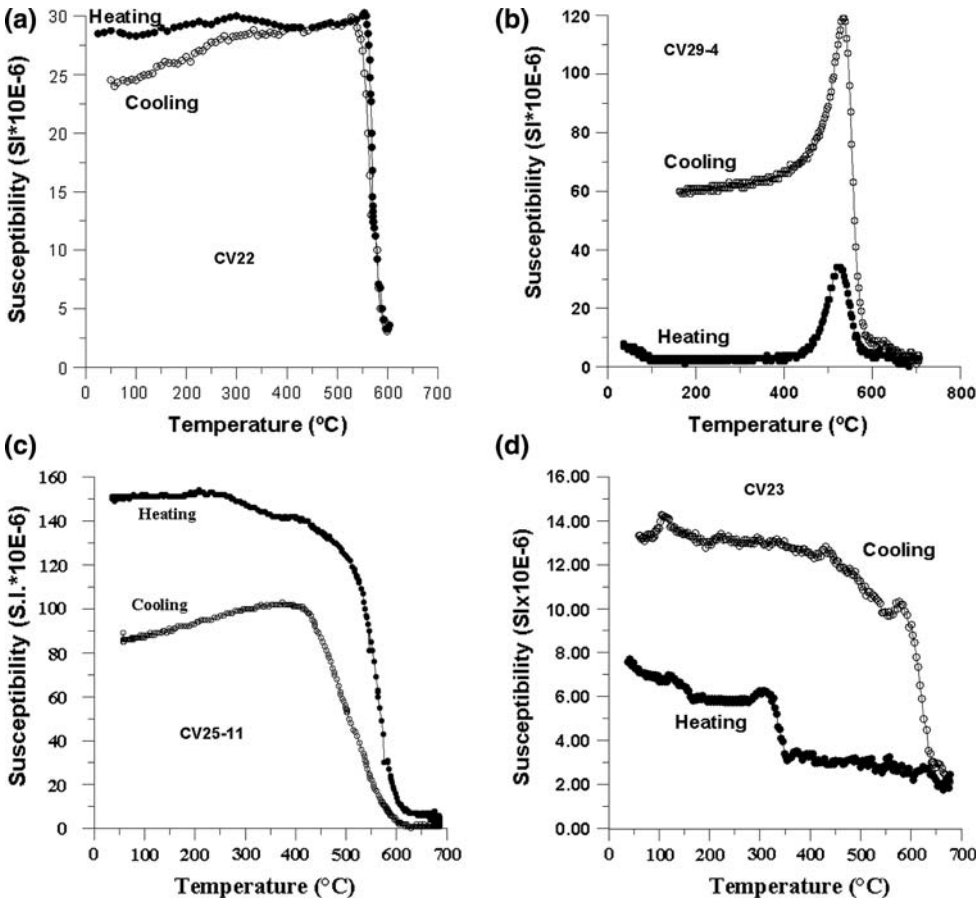


Fig. 2 Susceptibility versus temperature curves. Four examples (**a**, **b**, **c**, **d**) of *k–T* curves described in the text. *Solid symbols* are for heating curves, *open symbols* for cooling curves

samples share a large enhancement of susceptibility values in cooling curves, related to creation of magnetite during heating, although a small amount of this mineral could be already present in the samples. Samples CV35 and CV37 may also carry a minor fraction of pyrrhotite, although these observations should be regarded with care, as susceptibility variations lie near the noise-level of the susceptibility-meter.

In order to obtain information about the domain state of the studied samples, measurements of hysteresis parameters were carried out at room temperature on samples from seven of the studied volcanic sites with a Micromag 2900 alternating gradient magnetometer. With this device, a maximum field of 1.4 T can be applied. When hysteresis parameters are represented in a modified Day-plot (Day et al. 1977; Dunlop 2002a, b), they show PSD structure, with site CV24 tending towards SD domain structure (Fig. 3; Table 1).

Measurements of anisotropy of magnetic susceptibility (AMS) were carried out on 29 samples of 7 of the studied volcanic sites with a KLY-2 Kappabridge. Anisotropy factor P shows low to moderate values (Table 1), with a maximum in site CV21, in which P amounts to 1.069.

Ore microscopic studies on polished sections were carried out with a LEITZ microscope on 17 samples from 7 sites, with a maximum augmentation of 100×. Samples from sites CV21, CV22, CV24 and CV27 show slight traces of hydrothermal alteration while samples from CV23 and CV25 are characterised by stronger alteration. As it will be shown later, these results are basically in agreement with the paleomagnetic behaviour observed during demagnetisation. In CV26, both less and more hydrothermally altered specimens were observed.

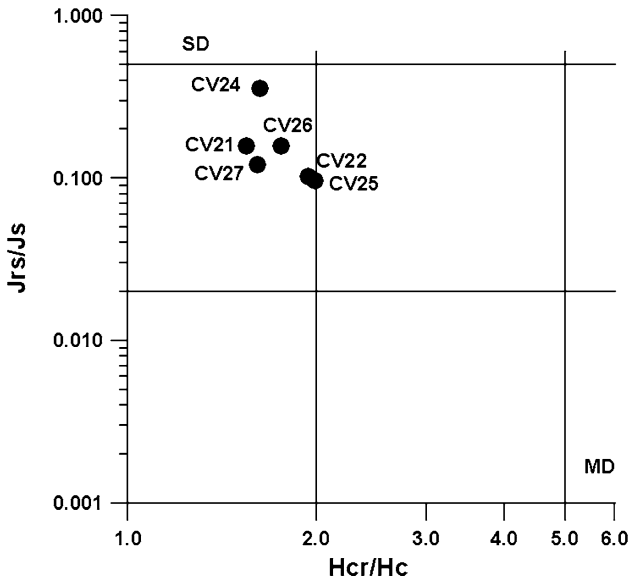


Fig. 3 M_{rs}/M_s versus H_{cr}/H_c plot of samples from the Basque Arc. Hysteresis parameter ratios of six samples from the Basque Arc. Data are represented in a Day-plot (Day et al. 1977) modified after Dunlop (2002a). Both axes are represented in a logarithmic scale

Analysis of paleomagnetic experiments

NRM intensities of volcanic samples show differing values (Table 1), with mean intensities varying between two orders of magnitude (10^{-3}–10^{-5} $Am^2\,kg^{-1}$, approximately 1–10^{-2} Am^{-1}), while mean intensities of sedimentary sites display values of an order of magnitude of 10^{-6}–10^{-8} $Am^2\,kg^{-1}$ (approximately 10^{-3}–10^{-5} Am^{-1}). NRM directions also show a differing behaviour, with some sites characterised by great scatter and others displaying well-grouped directions (Table 2).

No fold test could be performed in most sites, but comparison of bedding corrected and non-corrected directions was helpful in analysing the time of remanence acquisition, as dip values were steep (in almost all cases between 40 and 140°).

Demagnetisation behaviour during paleomagnetic experiments varied depending on the site analysed. ChRM results are listed in Table 3. One site, CV28, did not provide coherent results. Volcanic sites CV21 and

Table 2 NRM results

Site	NC/NS	DEC	INC	k	α_{95}
CV21 (V)	12/15	16.6	12.6	31.8	7.8
CV22 (V)	11/13	3.4	13.1	1.7	51.9
CV23 (V)	12/17	103.5	72.7	2.9	31.0
CV24 (V)	12/14	30.8	63.2	14.3	11.9
CV25 (V)	10/14	318.2	28.6	10.3	15.8
CV26 (V)	10/11	350.6	56.0	201.3	3.4
CV27 (V)	13/13	221.3	53.6	81.9	4.6
CV28 (V)	10/19	24.7	13.2	5.3	23.3
CV29 (V)	10/20	351.6	5.6	50.4	6.9
CV30 (S)	7/8	4.3	24.6	46.1	9.0
CV31 (S)	8/8	291.2	–36.4	5.0	28.0
CV32 (S)	11/15	74.8	62.9	1.9	46.4
CV33 (S)	8/10	324.0	37.7	4.6	29.1
CV34 (S)	8/11	286.8	–56.3	2.0	54.0
CV35 (S)	9/13	342.3	56.3	29.2	9.7
CV36 (S)	10/13	320.9	89.1	3.0	33.5
CV37 (S)	10/14	64.4	–9.3	1.9	49.4
CV38A (S)	9/10	32.7	3.4	10.1	17.1
CV38B (S)	7/8	227.5	36.5	4.0	34.6

Site: *V* volcanic, *S* sedimentary site; NC/NS: number of studied cores/number of studied specimens (each core provides a single direction for calculation of the mean); DEC: declination; INC: inclination; k: precision parameter; α_{95}: radius of 95% confidence cone

Table 3 Characteristic component

Site	Age	NC/NS	Dir/Pln	DEC (NC)	INC (NC)	DEC (BC)	INC (BC)	k	α_{95}	SLAT (N)	SLON (E)
CV21 (V)	Coniacian–Santonian	12/15	12/0	17.0	12.3	355.3	52.9	122.7	3.9	43.2	–2.5
CV22 (V)	Coniacian–Santonian	11/13	11/0	2.1	3.4	348.3	39.3	101.1	4.6	43.2	–2.5
CV22 (V)[a]	Coniacian–Santonian	4/5	4/0	177.5	–1.0	165.1	–34.6	29.4	17.2	43.2	–2.5
CV23 (V)	Late Albian–Cenomanian	12/13	6/6	196.5	–9.4	185.0	–53.4	12.1	13.0	43.2	–2.4
CV24 (V)	Coniacian–Santonian	10/10	4/6	41.3	–4.4	39.3	46.0	44.9	7.3	43.2	–2.5
CV25 (V)	Late Albian–Cenomanian	10/13	10/0	314.9	13.3	56.8	59.2	36.6	8.1	43.4	–2.8
CV26 (V)[b]	Late Albian–Cenomanian	10/11	10/0	334.7	47.4	77.2	28.9	111.5	4.6	43.4	–2.8
CV27 (V)	Late Albian–Cenomanian	12/12	12/0	219.8	53.2	30.4	51.6	128.0	3.9	43.3	–3.0
CV28 (V)	Late Albian–Cenomanian	No coherent results									
CV29 (V)	Late Albian–Cenomanian	10/10	10/0	160.7	–33.6	199.5	–50.5	55.1	6.6	43.4	–2.8
CV30 (S)	Cenomanian	7/7	7/0	3.2	23.1	25.1	28.6	82.1	6.7	43.4	–2.8
CV31 (S)	Upper Cretaceous	10/11	10/0	337.8	49.4	291.6	49.0	42.1	7.5	43.2	–2.2
CV32 (S)	Upper Cretaceous	11/11	2/9	138.7	56.2	174.9	48.8	10.5	15.4	43.4	–3.0
CV33 (S)	Oxfordian	8/10	0/6	6.9	21.8	6.8	56.1	37.5[d]	14.3[d]	43.2	–2.2
CV34 (S)	Pliensbachian	8/11	8/0	225.7	–65.6	354.1	28.9	62.4	7.1	43.2	–2.2
CV35 (S)	Neocomian	9/13	0/7	353.1	30.4	11.4	68.0	37.8	12.1	43.2	–2.2
CV36 (S)	Ypresian	8/8	2/6	279.7	79.0	335.0	33.7	26.4	11.9	43.3	–2.1
CV37 (S)[b]	Upper Paleocene	10/13	0/10	173.7	–37.0	165.4	–7.2	3.7	30.4	43.3	–2.1
CV38A (S)	Upper Paleocene	8/9	8/0	59.8	–42.2	61.7	51.6	51.1	7.8	43.4	–3.0
CV38B (S)	Upper Paleocene	6/6	6/0	214.1	1.6	217.8	–58.2	35.7	11.4	43.4	–3.0
CV38 (S)[c]	Upper Paleocene	14/15	14/0	46.9	–25.7	52.5	55.0	33.0	7.0	43.4	–3.0
Sites from other studies											
SIM (S)	Triassic–Jurassic	13 (2 sites)				44.0	18.0		1.6		
SDE (S)	Late Albian	27 (5 sites)				359.6	45.1		3.4		
P1995 (S)	Late Maastrichtian–Paleocene	104		189	16	7	39	12[d]	4.2[d]		
DT2002 (S)	Danian–Selandian	74				11.7	47.4	7.2	6.6	42.3	–2.3
DT2003 (S)	Paleocene–Eocene boundary	171				17.1	42.6	8.1	4.0	42.3	–2.3

Site: *V* volcanic, *S* sedimentary site; Paleomagnetic results from previous studies (see text): SIM, SDE (Vandenberg 1980), P1995 (Pujalte et al. 1995), DT2002 (Dinarès-Turell et al. 2002) and DT2003 (Dinarès-Turell et al. 2003); Age: age of each site; NC/NS: number of studied cores/number of studied specimens (each core provides a single direction for calculation of the mean), results from previous studies are given only with the number of samples; DIR/PLN: number of directly determined directions and planes employed for calculation of the mean direction (after McFadden and McElhinny 1988); DEC and INC (NC): declination and inclination given in non-tilt-corrected coordinates; DEC and INC (BC): declination and inclination, data given in tilt corrected coordinates; k: precision parameter; α_{95}: radius of 95% confidence cone. SLAT and SLON: longitude (north) and latitude (east) of each site

[a] Second ChRM component of CV22, see text

[b] Sites excluded from tectonic interpretation, see text (CV26, CV32, CV37)

[c] Result of combining data from CV38A and B (positive fold test, see text)

[d] Non-corrected and bedding corrected directions of sites CV33 and P1995 yield different k and α_{95} values, the latter are indicated in the table

CV27, as well as sedimentary site CV30 showed the simplest behaviour, characterised by a normal-polarity paleomagnetic component mainly carried by magnetite (Fig. 4a, b). The same was observed in most samples from CV22, but 4 of the 11 samples studied in this site also carried a low-temperature (unblocking temperatures $T_{UB} < 300°C$) reversed-polarity component, which has the same direction than the normal-polarity direction. In the other samples belonging to CV22 only a viscous component could be recognised in the low-temperature range. Comparison of paleodirections of these volcanic sites before and after bedding correction suggests that characteristic remanence (including the reversed low-temperature component of CV22) has been acquired before rotations about horizontal axes took place, as the uncorrected directions show anomalous values much more difficult to explain than the corrected ones (Table 3). In sedimentary site CV30, however, the characteristic component might have been acquired before or after tilting.

Both CV26 and CV25 show the presence of two paleomagnetic components, one of them carried by low-Ti titanomagnetite, the latter site in accordance with the behaviour observed in k–T curves. As in the cases discussed above, no fold test was possible and again paleodirections before and after bedding correction were compared. In CV25, the uncorrected low-temperature component shows a present-day direction, while the high-temperature component, which was isolated between 200/400 and 500°C, depending on the

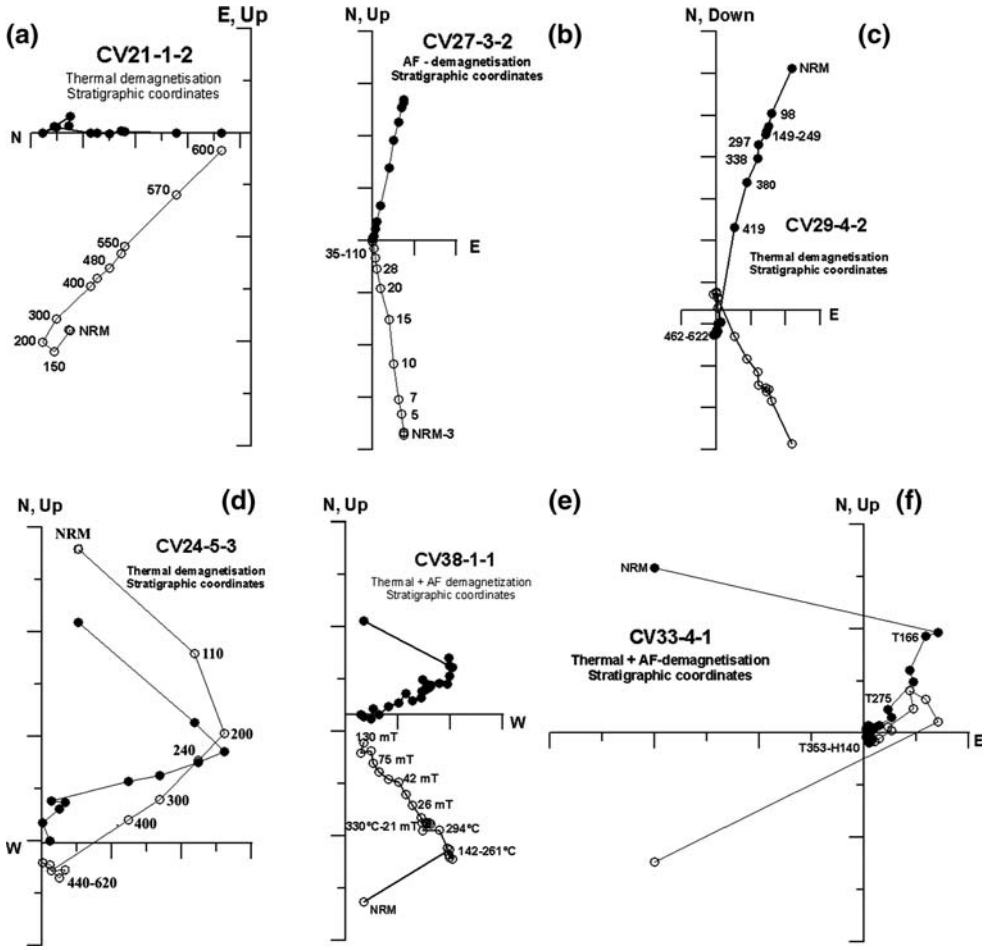


Fig. 4 Orthogonal demagnetisation plots. Four examples of thermal (**a**, **c**, **d**) and AF (**b**) demagnetization of volcanic specimens and two examples of combined thermal + AF demagnetization of sedimentary specimens (**e**, **f**). *Solid symbols* show projections of vector endpoints onto the horizontal plane, *open symbols* onto the vertical plane. Figures on the curves give demagnetisation temperatures in °C or demagnetization fields in mT. In combined demagnetization plots, a *T*-label indicates a thermal demagnetization step and an *H*-label indicates an AF demagnetization step. In all six cases bedding-corrected data are shown

degree of overlapping between both components, seems to have been acquired prior to tilting (Table 3). In CV26, however, both paleomagnetic components seem to have been acquired after tilting, as inferred from the meaningless value of the corrected direction. The first one is a present-day direction and the second, which could be isolated between 400 and 580°C, displays a NNW declination.

Paleomagnetic analysis of sites CV23, CV24 and CV29 was less straightforward. In CV23, a reversed-polarity ChRM, mainly carried by pyrrothite (also recognised in the *k*–*T* curve) was found, which apparently had been acquired before tilting, as inferred from the anomalous value of the uncorrected direction. Due to the presence of a viscous component visible at demagnetisation temperatures below 220°C and to chemical/mineralogical alterations caused by heating, the ChRM component was difficult to determine. If the site mean direction is calculated by taking only the directly determined directions, a result of $D = 194°$, $I = -49°$ ($\alpha_{95} = 18$, $N = 9$) is obtained. However, as some of these directly determined directions were calculated from only a low number of points, we choose to combine those directions of better quality with remagnetisation circles (McFadden and McElhinny 1988) obtained from the demagnetisation of the rest, and were much better defined than the ChRM directions, arriving to the following result: $D = 185°$, $I = -53°$ ($\alpha_{95} = 12$, $N = 12$; Table 3).

Site CV29 displayed two paleomagnetic components (Fig. 4c): A component which in most cases shows unblocking temperatures between 300/400°C and 530/590°C and displays normal polarity after bedding correction, while before correction its mean inclination is nearly horizontal, and a reversed-polarity component (both with and without bedding correction) with unblocking temperatures between 560/590°C and 620/660°C, in accordance with *k*–*T* data. As this site is of Cenomanian age, Albian and late Cretaceous paleomagnetic directions for the Eurasian plate were calculated from the synthetic APWP determined by Besse and Courtillot (2002) and its inclinations compared with inclinations of the high-temperature component (HT) before (–34 ± 5°) and after bedding correction (–51 ± 5°). All 5 Ma time-windows considered between 70 and 110 Ma showed an agreement with the

bedding-corrected inclination, but not with the uncorrected, so that we consider that it is more likely that the HT-component was acquired prior to tilting, although the effect of secular variation should be taken into account for a single volcanic site. The normal polarity component, characterised by a low inclination, probably does not correspond to a real palaeomagnetic component, but to two overlapping ones of opposed polarity, one of them being the previously mentioned high temperature component. This interpretation is supported by the fact that if the initial stretch of demagnetisation plots is analysed, although the obtained directions are relatively poorly defined, a normal-polarity direction can be obtained, which after bedding correction is in accordance with the previously mentioned expected Albian–late Cretaceous paleodirections ($D = 8.2°$, $I = 45.4°$, $\alpha_{95} = 14$, $N = 9$).

In site CV24, besides a viscous present-day component, two other ones could be recognised (Fig. 4d). A first one (component A) could be determined at demagnetisation temperatures between 200/400 and 500/600°C, displayed a normal polarity in nine and reversed polarity in three of the studied cores and probably has a secondary origin, having been acquired after tilting, as can be inferred from the analysis of the paleoinclinations obtained. The second component (component B) is difficult to isolate, and can be directly determined in only four samples, being poorly defined by few points in the 550–620°C demagnetisation interval. It should be noted that at this latter temperature, most samples were completely demagnetised. The inclination shown by component B is nearly horizontal before bedding correction and agrees with the expected Albian–late Cretaceous ones after bedding correction ($D = 37.6°$, $I = 44.6°$, $\alpha_{95} = 22$, $N = 4$), so that we consider that it is more likely that remanence was acquired prior to tilting. Analysis of the directional behaviour of samples from this site during demagnetisation showed that paleomagnetic directions lie on great circles and tend towards a NE declination in bedding corrected coordinates, agreeing with the directly determined declination of component B. The mean paleomagnetic direction of component B (Table 3) was calculated by combining directly determined directions with remagnetisation circles (McFadden and McElhinny 1988) (Fig. 5).

Demagnetisation of samples from CV31 unveiled the presence of two components, a present-day one and a second one carried by magnetite, which shows a westward deviated paleodeclination, regardless of whether it is considered to have been acquired before ($D = 291.6°$, $I = 49.0°$) or after tilting ($D = 337.8°$, $I = 49.4°$). In sites CV38A and CV38B, a paleomagnetic component could be isolated between approximately 150 and 400°C or above 15 mT, and was best recognised in samples subjected to both thermal and AF-cleaning (Fig. 4e). A positive fold test (McElhinny 1964) confirmed that the observed paleomagnetic component is pre-fold at a 99% level ($k_{after}/k_{before} = 3.5$).

In sites CV32, CV36 and CV37, which were characterised by very low intensities, ChRM directions could only be obtained by combining directly determined directions with remagnetisation circles (McFadden and McElhinny 1988). In CV36, a counterclockwise rotated normal-polarity direction was obtained combining six remagnetisation circles with two directly determined directions. As with this method the finally calculated mean direction is biased towards the directly determined directions, the calculated mean was compared with the mean direction obtained only from remagnetisation circles, both directions showing agreement. By simple comparison of the corrected and uncorrected directions, it could not be decided, however, whether this component was acquired prior to or after tilting of the bedding plane. In CV32, a mean paleomagnetic direction was obtained after combining two directly determined directions with nine remagnetisation circles, the result also being confirmed by comparison with a direction obtained only from remagnetisation circles. A strongly rotated paleodeclination is observed, both if the paleomagnetic

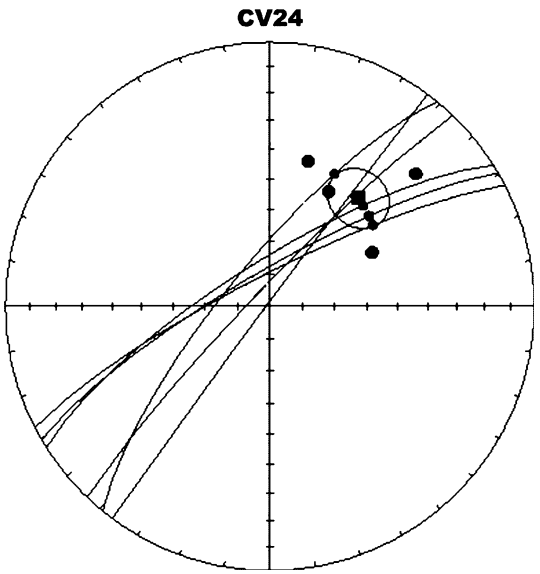


Fig. 5 Mean direction of site CV24. Combination of directly determined directions with remagnetisation circles (after McFadden and McElhinny 1988) obtained from demagnetisation experiments in site CV24 (see text). *Small dots* Directly determined directions; *large dots* directions obtained from remagnetisation circles

component has been acquired before ($D = 175°$) or after ($D = 139°$) tilting. However, due to the low quality of the demagnetisation data of this site, results should be considered with care. In CV37, a combination of directly determined directions and remagnetisation circles provided a low-quality reversed polarity direction, most probably acquired after tilting as can be ascertained by comparison of the bedding-corrected and non-corrected result.

Jurassic to lower Cretaceous sites CV33, CV34 and CV35 are all located in the same area. In CV34, besides a viscous low-temperature component, an intermediate-temperature component below 362°C and a high-temperature (and high unblocking field) component were found. If bedding corrected, a normal-polarity direction was obtained from the intermediate-temperature component, but the direction of the high temperature component could not be determined. In sites CV33 (Fig. 4f) and CV35 no coincidence was observed between directions of samples from the same site, probably due to overlapping of components, but remagnetisation circles provided northwards directed normal-polarity directions. In CV33, however, different bedding corrections had to be applied to different groups of samples, and bedding corrected directions were significantly better grouped ($k_{after}/k_{before} = 2.4$).

Discussion and conclusions

As shown by the previous discussion, analysis of demagnetisation behaviour provided paleomagnetic directions in all but one site, as only in CV28 no coherent results could be determined. The question to be posed is whether results obtained correspond to primary paleodirections. As previously mentioned, no fold test could be performed in most sites, although in site CV38 a positive fold-test assures that the paleomagnetic direction obtained was acquired prior to folding, and thus might be primary. A similar argument may be employed for site CV33. Comparison of bedding corrected and non-corrected directions was helpful in analysing the time of remanence acquisition, as angular differences of the directions of the bedding planes were large, and dips were characterised by steep values. As shown in Table 3 and discussed in the previous section, this kind of analysis suggests that in many of the studied sites remanent magnetisation might have been acquired before tilting of the bedding planes. Although this kind of analysis can provide useful qualitative information, conclusions regarding the time of remanence acquisition inferred that way should be taken with care, as they generally cannot be considered reliable. Although no fold test information was available in most cases, when the large angular differences of the bedding plane directions are considered, performance of a regional fold test appears as a possible alternative. With this purpose, the mean direction of uncorrected and bedding-corrected ChRM directions of the studied sites was calculated. A positive fold test ($k_{after}/k_{before} = 2.5$) seems to confirm that remanence was acquired before dipping of bedding planes took place, when all 19 sites providing ChRM results are considered. If the same calculation is performed excluding three sites (CV37 because of the great scatter of directions observed, with $k = 3.7$, CV26 because comparison of uncorrected and corrected ChRM clearly points to a remagnetised paleomagnetic direction and CV32 because of the low quality of its demagnetisation data and its anomalous direction both if corrected or uncorrected), the result (Fig. 6) is a much clearer positive fold test ($k_{after}/k_{before} = 4.9$) at a 99% level (McElhinny 1964). The three mentioned sites have been excluded from further analysis.

In spite of this positive fold test, the scatter of mean directions of these 16 bedding-corrected sites is still considerable ($k = 11.9$, $\alpha_{95} = 11.2$). If declination and inclination data are analysed, it can be observed that while declination results vary between 292 and 56°, inclination values only fluctuate between 29 and 68° (Fig. 6; Table 3). This result points to the occurrence of vertical axis rotations. In that case, results of a positive regional fold test could be obscured by an extra scatter in declination. Considering the strike of the axial planes of the main folds in the Basque Arc (Table 4), the studied area has been subdivided into three different sectors: A western sector including sites CV25, CV27, CV29, CV30, CV38A and CV38B, a central sector with sites CV21, CV22 (with two ChRM components), CV23, CV24, CV33, CV34 and CV35 and an eastern sector with the two easternmost sites CV31 and CV36 which, unlike the other sites, display significantly counter-clockwise rotated paleodeclinations. The latter two sites are located at a similar longitude than sites CV33, CV34 and CV35, which have been ascribed to the central sector, and their different behaviour can be explained by the fact that they are located in the inner side of the Basque Arc, while the other sites are on its outer side. As the length of the hinge zone of a fold decreases from the outer to the inner arc of a fold, a small eastward displacement with respect to the axial plane of the arc would be enough to shift sites CV31 and CV36 to the eastern branch of the Basque Arc. Instead of performing a regional fold test for the whole studied area, fold tests can also been carried out considering only the sites included in a sector. This

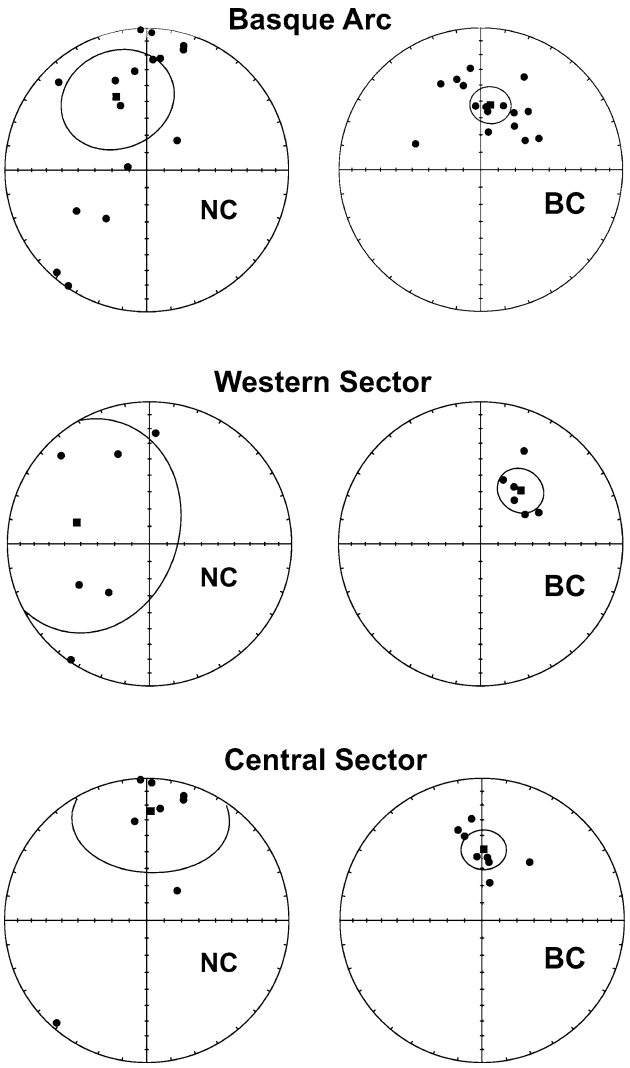


Fig. 6 Regional fold tests. Comparison of ChRM directions without (NC) and with (BC) bedding correction for the whole Basque Arc as well as the western and the central sectors (see text). Sites CV26, CV32 and CV37 are not included (see text). *Solid circles* show mean site directions, *solid squares* show mean sector directions, *ellipses* show α_{95} confidence cones

analysis has only been carried out in the western and central sectors, as there are only two single sites available in the eastern sector. Positive fold tests confirm, in both cases (Fig. 6, western sector $k_{after}/k_{before} = 12.5$; central sector $k_{after}/k_{before} = 7.3$), that the observed paleomagnetic component is pre-fold at a 99% level (McElhinny 1964).

In addition, the possibility of a syn-folding magnetisation was also checked for both the western and the central sector. In Fig. 7, variation of ChRM directions during unfolding in each of the sectors is shown. For this kind of analysis, only one of the ChRM directions obtained in CV22 was considered because both directions come from the same site and thus share the same bedding correction. CV33 was excluded because, in that site, different bedding corrections had to be applied to different sample groups, each one consisting of only a small amount of samples. Therefore, only six sites were available in the central sector. ChRM directions from each site plot on small circles during unfolding, and the resulting best-fitting directions in both analysed sectors (Fig. 7), obtained following the SCI-method proposed by Shipunov (1997) and modified by Waldhör and Appel (2006), suggest that the studied sites posses a ChRM acquired before tilting of the bedding planes. Only in sites CV38B in the western sector and CV35 in the central sector, a syn-folding ChRM acquisition appears to be possible following this kind of analysis. Taking that possibility into account, however, would leave paleodeclinations almost (CV35) or completely (CV38B) unchanged.

A question which can be still be posed is if ChRM directions are primary palaeodirections. It does not seem very probable that the reversed-polarity directions (CV23, CV29, one of the components from CV22) correspond to primary paleomagnetic components. The Albian to Santonian age of all studied volcanic sites, except perhaps CV31, coincides with the Cretaceous Normal Polarity Superchron (CNPS), during which only few brief reverse-polarity subchrons might have occurred (Gradstein et al. 1994). On the other hand, M_{SR}/M_S ratios of samples from several volcanic sites correspond to a PSD domain structure, and hysteresis parameters on a modified Day plot (Day et al. 1977; Dunlop 2002a, b) display a PSD behaviour,

Table 4 Palaeomagnetic directions of sectors of the Basque Arc

Sector	Site	Strike	*N*	DEC	INC	*k*	α_{95}	ΔD
West		120°	6	37.0	44.7	17.6	16.4	18
Central		100°	12	4.1	47.0	30.7	8.0	9
East	CV31	60°	10	291.6	49.0	42.1	7.5	9
	CV36		8	335.0	33.7	26.4	11.9	11

Sector: Subdivision of the Basque Arc (see text); site: in the eastern sector, site name; *N*: number of palaeomagnetic directions used for calculation of the sector mean direction, in the eastern sector, number of cores used to determine mean direction; Strike: mean strike of axial planes of main folds from each of the three sectors; DEC: declination; INC: inclination; *k*: precision parameter; α_{95}: radius of 95% confidence cone; ΔD: confidence limit for declination (calculated after Demarest 1983)

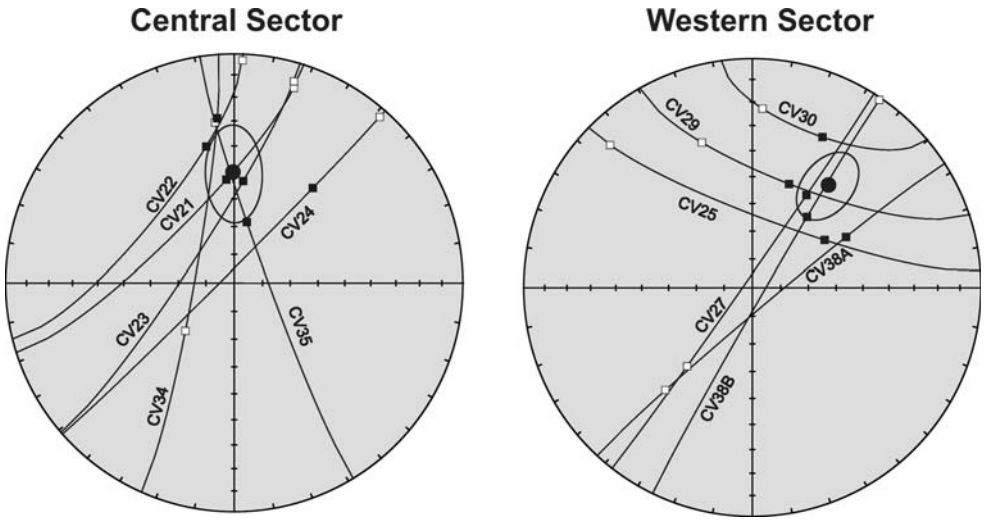


Fig. 7 Regional fold tests. Analysis of the possibility of syn-folding acquisition of remanence. Regional fold tests in the western and central sectors (see text). Analysis of the possibility of syn-folding acquisition of remanence. ChRM directions of each site during unfolding plot on small circles. *White squares* show uncorrected ChRM directions, *black squares* show ChRM values after complete bedding correction. *Solid circles* show estimated mean ChRM direction, which was obtained following the method proposed by Shipunov (1997) and modified by Waldhör and Appel (2006)

with site CV24 tending towards SD domain structure (Fig. 3; Table 1). In addition, *k–T* curves of volcanic sites CV21, CV22, CV24 and CV27 show high thermal stability and ore microscopic analysis of these sites shows only slight traces of alteration. These results point to a primary origin of the normal polarity components of the volcanic sites. However, even if the obtained paleodirections do not correspond to a primary direction, they seem to have been acquired prior to tilting, as previously discussed. On the other hand, possible rotations about horizontal or vertical axes must have occurred later, due to post-Lutetian (49.0–41.3 Ma) compressive tectonics, which resulted in the Pyrenean orogeny.

As site CV28 did not provide coherent results, sites CV26, CV32 and CV37 have been excluded from further analysis, two different paleodirections have been obtained in CV22, and CV38A and CV38B together provide a single one, 15 paleomagnetic directions are available for interpretation. In addition, results from previous paleomagnetic studies in the Basque-Cantabrian basin have been considered for further discussion, like the paleomagnetic directions obtained in the magnetostratigraphic studies carried out by Pujalte et al. (1995), Dinarès-Turell et al. (2002) and Dinarès-Turell et al. (2003) as well as the paleodirections of sites SDE (Deba) and SIM (Gernika) from Vandenberg (1980). Results from other magnetostratigraphic studies in the Basque Arc were rejected because (1) demagnetisation was performed with a single step at 400°C (Roggenthen 1976); (2) directions of characteristic remanence were difficult to determine accurately (although polarity was clearly assessed) and a present earth field overprint significantly contaminated the original magnetisation (Mary et al. 1991) and (3) a significant scatter due to rotations about the axes of the cores is observed (Moreau et al. 1994). In the two latter magnetostratigraphic studies, the arguments given here for rejection are discussed by the authors themselves. Both studies were carried out on the Cretaceous/Tertiary Sopelana section, and in the present study we have sampled sites CV38A and CV38B in that location. Both sites are located on both limbs of a single fold, so that a fold test could be performed.

If the 15 paleodeclinations obtained in the present study together with the results from the mentioned five other previous studies are analysed individually as a function of their geographic position, in order to find out if they provide any clue about the primary or secondary origin of the Basque Arc, no significant correlation can be recognised between site location and declination value. Nevertheless, as many results were obtained from volcanic sites, the effect of secular variation has to be taken into account. Therefore, paleomagnetic results should be considered in groups instead of individually. As already discussed, the studied area was divided into a western, a central and an eastern sector. In addition to the previously mentioned sites from the present study, site SIM from Vandenberg (1980) was included in the western sector, while site SDE from Vandenberg (1980), as well as

results from three magnetostratigraphic studies (Pujalte et al. 1995; Dinarès-Turell et al. 2002, 2003) were included in the central sector.

The results obtained are shown in Fig. 8 and Table 4**.** While inclinations of all three sectors show a similar value, declinations differ. The western sector displays a 37 ± 16° clockwise rotation of its mean paleodeclination, the central sector is not rotated (4 ± 9°) and both sedimentary sites which make up the eastern sector show counter-clockwise rotations (–25 ± 11° and –68 ± 9°). It should be borne in mind that ages of the sites considered vary between upper Paleocene and Triassic/Jurassic. Nevertheless, if expected directions are calculated from the synthetic APWP for Eurasia (Besse and Courtillot 2002), paleodeclinations vary only slightly between approximately 2 and 6° for the sites younger than Oxfordian, and an expected declination of 11° is obtained for the latter age. Two of the studied sites, however, CV34 and SIM from Vandenberg (1980) have older early Jurassic/Triassic ages, and their expected paleodeclinations display values of approximately 29°. Excluding both sites from the calculated means would yield virtually the same values, 35 ± 19° in the western sector and 5 ± 10° in the central sector, reflecting that remanence in these sites, although pre-fold, perhaps is not primary. For further analysis we will consider the mean directions without excluding sites CV34 and SIM.

Although paleodeclination results of the sectors are in accordance with the trend of the strike of the axial planes of the main folds in the Basque Arc, confidence limits display relatively high values (Table 4). In order to find out if the mean directions obtained in the western and central sectors are different (i.e. if both data sets share a common mean direction), we applied the test proposed by McFadden and Lowes (1981) coming to the result that both directions are different at a 95% level of confidence. The paleomagnetic directions of the eastern sector, being obtained from two sedimentary sites, should not reflect the perturbing effect of secular variation and are clearly different from the directions of the western and central sectors. Thus, paleomagnetic results from the present study suggest that the arched shape of the Basque Arc has not a primary origin, but a secondary origin due to rotations about vertical axes as a result of the differential shortening related to post-Lutetian compressive tectonics which resulted in the formation of the Pyrenees. The strike of the axial planes of the main folds of the Basque Arc, which varies from N120° in the west to N100° in its central part and N60° in the East, roughly agrees with the amount of paleomagnetic rotation observed in the present study in the western, central and eastern sectors.

It should be borne in mind, however, that the amount of available paleomagnetic data, particularly in the eastern sector, is low, and that some sites were characterised by a complex paleomagnetic behaviour, so that quantitative interpretations of these results should be regarded with care.

Paleomagnetic directions of sedimentary sites CV33 (Oxfordian, late Jurassic), CV34 (Pliensbachian, early Jurassic) and CV35 (Neocomian, lower Cretaceous), which are all located in the central sector, and thus

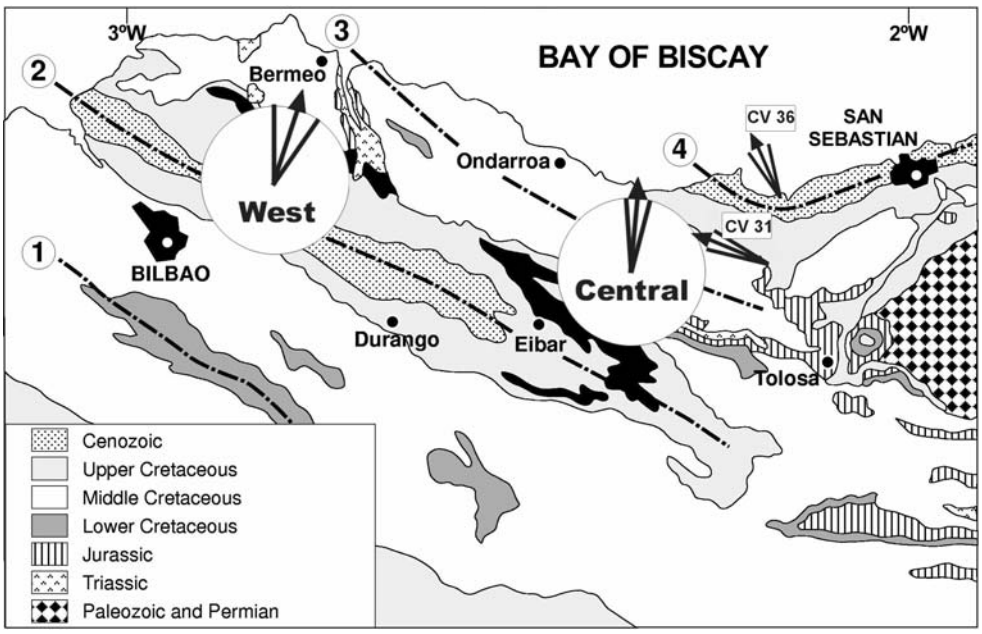


Fig. 8 Paleodeclination results. Schematic geological map of the Basque Arc with location of sampled sites. Mean paleodeclinations of the western and central sectors (see text) with confidence limits (calculated after Demarest 1983) and paleodeclinations of two sites (CV31 and CV36) belonging to the eastern sector are shown

have probably not experienced vertical-axis rotations, were compared with the expected directions of Iberia and Eurasia. The expected Iberian Oxfordian direction was calculated from two Oxfordian poles (Steiner et al. 1985; Juárez et al. 1998), an expected Pliensbachian Iberian direction from four early Jurassic poles (Osete et al. 2000; Schott et al. 1981; Palencia 2005) and an expected Neocomian Iberian direction from three Neocomian poles (Galdeano et al. 1989; Moreau et al. 1997; Galbrun et al. 1990). Expected European directions for these ages were obtained from different 5 My time-windows from the synthetic European APWP calculated by Besse and Courtillot (2002). Comparison of the paleodirection of Oxfordian site CV33 yields an angular difference of 7° with the expected European direction obtained from the 155 My window and 30° with the expected Iberian direction, thus showing a better agreement with the European direction. The paleomagnetic direction from site CV35 also shows a much better agreement with the expected European direction, displaying a 26° angular difference with the expected Iberian direction and a 6° angular difference with the expected European direction obtained from the 130 My window. In site CV34, however, no good agreement is observed neither with the expected results from the European nor the Iberian plate, as angular differences of 34° with the former and 25° with the latter are observed. These discrepancies could be due to a non-primary character of its ChRM.

This result may have different explanations: (a) the observed direction could be a post-Jurassic but pre-folding remagnetisation, so that the counter-clockwise rotation of Iberia would not be recorded in it; (b) the observed data reflect the Basque Arc that did not form part of Iberia, but of Eurasia during rotation of the Iberian Peninsula; (c) local clockwise rotations could balance Iberia's counter-clockwise rotation. This latter possibility would be, however, a less probable coincidence.

If we consider sites CV33 and CV35, which are located in the central sector are neither rotated nor remagnetised, their paleomagnetic results would be in accordance with conclusions drawn from recent tectonic, metamorphic (Cuevas and Tubía 1999) and seismic data (Pedreira et al. 2003) obtained in the Basque Arc, which corroborate that the Basque Arc belongs to the NPZ and consequently is related to the European plate. Paleomagnetic information obtained from only two sites, however, is clearly insufficient to support this interpretation. Unfortunately, sites of a suitable age (older than Aptian) are very scarce in the studied region.

Acknowledgments We are grateful to E. Pueyo and R. Scholger for their helpful and constructive reviews as well as to R. van der Voo for his useful comments to a former version of the manuscript. This work was supported by projects BTE2002-04168-C03 and CGL2004-00701 from the Spanish Ministry of Science and Technology, projects BU16/03 and BU 30/04 of the Junta de Castilla y León, and grant Grupos consolidados de investigación de la Universidad del País Vasco.

References

Azambre B, Rossy M (1976) Le magmatisme alcalin d'âge crétacé dans les Pyrénées occidentales et l'Arc basque; ses rélations avec le métamorphisme et la tectonique. Bull Soc Geol Fr 7(18):1725–1728

Besse J, Courtillot V (2002) Apparent and true polar wander and the geometry of the geomagnetic field over the last 200 Myr. J Geophys Res 107 (B11):2300. DOI 10.1029/2000JB000050

Boillot G, Capdevila R, Hennequin-Marchand I, Lamboy M, Lepetre JP (1973) La zone nord-pyrénéenne, ses prolongements sur la marge continentale nord-espagnole et sa signification structurale. C R Acad Sci Paris 277:2692–2632

Brinkmann R, Lögters H (1968) Diapirs in western Pyrenees and foreland, Spain. In: Braustein J, O'Brien GD (eds) Diapirism and diapers. AAPG Mem 8:275–292

Cabanis JA, Le Furt-Balouet S (1990) Le magmatisme Crétacé des Pyrénées. Apport de la géochimie des éléments en traces Consequences chronologiques et géodynamiques. Bull Cent Explor Prod Elf-Aquitaine 14:155–184

Choukroune P (1976) Structure et évolution téctonique de la zone nordpyrénéenne (analyse de la déformation dans une portion de chaîne à schistosité subverticale). Mem Soc Géol Fr 127:1–116

Choukroune P, Mattauer M (1978) Tectonique des plaques et Pyrénées: sur le fonctionnement de la faille transformante nord-pyrénéenne; comparaison avec des modèles actuels. Bull Soc Géol Fr 5:689–700

Choukroune P, Seguret M, Galdeano A (1973) Caractéristiques et evolution structurale des Pyrénées. Bull Soc Géol Fr 15:601–611

Cuevas J (1979) Estudio petrográfico del vulcanismo intercalado en el Cretácico, entre los ríos Urola y Deva (Guipúzcoa). Tesis de Licenciatura, Univ. de Bilbao, p 107

Cuevas J, Tubía JM (1999) The discovery of scapolite marbles in the Biscay Synclinorium (Basque-Cantabrian basin, western Pyrenees): geodynamic implications. Terra Nova 11:259–265

Cuevas J, Eguiluz L, Ramón-Lluch R, Tubía JM (1982) Sobre la existencia de una deformación tectónica compleja en el flanco N del sinclinal de Oiz-Punta Galea. Nota preliminar. Lurralde. Investigación y espacio, pp 47–61

Cuevas J, Aranguren A, Badillo JM, Tubía JM (1999) Estudio estructural del sector central del Arco Vasco (Cuenca Vasco-Cantábrica). Bol Geol Min España 110:3–18

Day R, Fuller M, Schmidt VA (1977) Hysteresis properties of titanomagnetites: grain size and compositional dependence. Phys Earth Planet Int 13:260–267

Demarest HH (1983) Error analysis for the determination of tectonic rotation from paleomagnetic data. J Geophys Res 105:19405–19418

Dinarès-Turell J, Baceta JI, Pujalte V, Orue-Etxebarría X, Bernaola G (2002) Magnetostratigraphic and cyclostratigraphic calibration of a prospective Paleocene/Eocene stratotype at Zumaia (Basque Basin, northern Spain). Terra Nova 14(5):371–378

Dinarès-Turell J, Baceta JI, Pujalte V, Orue-Etxebarría X, Bernaola G, Lorito S (2003) Untangling the Paleocene climatic rythm: an astronomically calibrated early Paleocene magnetostratigraphy and biostratigraphy at Zumaia (Basque Basin, northern Spain). Earth Planet Sci Lett 216:483–500

Dunlop DJ (2002a) Theory and application of the Day plot (Mrs/Ms versus Hcr/Hc) 1: theoretical curves and tests using titanomagnetite data. J Geophys Res 107(B3). DOI 10.1029/2001JB000486

Dunlop DJ (2002b) Theory and application of the Day plot (Mrs/Ms versus Hcr/Hc) 2: application to data for rocks, sediments and soils. J Geophys Res 107(B3). DOI 10.1029/2001JB000487

EVE (1995) Mapa geológico del País Vasco, escala 1: 100.000. Bilbao

Feuillée P, Rat P (1971) Structures et paléogéographies pyrénéo-cantabriques. In: Debyser J, Le Pichon X, Montadert L (eds) Histoire structurale du Golfe de Gascogne. Ed. Technip, París, pp 1.1–1.48

Galbrun B, Berthou PY, Moussin C, Azema J (1990) Magnétostratigraphie de la limite Jurassique-Cretàcé en las faciés de plateforme carbonatèe: la coupe de Bias do Norte (Algarve, Portugal). Bull Soc Geól Fr 8(VII):133–143

Galdeano A, Moreau MG, Pozzi JP, Berthou JA (1989) New paleomagnetic results from Cretaceous sediments near Lisboa (Portugal) and its implications for the rotation of Iberia. Earth Planet Sci Lett 92:95–106

Golberg JM, Leyreloup A (1990) High temperature–low pressure Cretaceous metamorphism related to the crustal thinning (eastern north Pyrenean zone, France). Contrib Mineral Petrol 104:194–207

Gradstein FM, Agterberg FP, Ogg JG, Hardenbol J, Van Veen P, Thierry J, Huang Z (1994) A Mesozoic timescale. J Geophys Res 99(B12):24051–24074

Gómez M, Vergés J, Riaza C (2002) Inversion tectonics of the northen margin of the Basque Cantabrian Basin. Bull Soc Géol Fr 173:449–459

Juárez MT, Lowrie W, Osete ML, Meléndez G (1998) Evidence of widespread cretaceous remagnetisation in the Iberian Range and its relation with the rotation of Iberia. Earth Planet Sci Lett 3–4:729–743

Kirschvink JL (1980) The least squares line and plane and the analysis of paleomagnetic data. Geophys J R Astron Soc 62:699–718

Lamolda MA, Mathey B, Rossy M, Sigal J (1983) La edad del vulcanismo de Vizcaya y Guipúzcoa. Estudios Geol 39:151–155

Larrasoaña JC, Parés JM, Valle J, Millán H (2003a) Triassic paleomagnetism from the Western Pyrenees revisited: implications for the Iberian-Eurasian Mesozoic plate boundary. Tectonophysics 362:161–182

Larrasoaña JC, Parés JM, Millán H, Valle J, Pueyo E (2003b) Paleomagnetic, structural and stratigraphic constraints on transverse fault kinematics during basin inversión: The Pamplona Fault (Pyrenees, north Spain). Tectonics 20(6). DOI 10.1029/2002TC001446

Lefort JP, Agarwal BNP (1999) Of what is the Ibero-Armorican arc composed? Tectonophysics 302:71–81

Malod JA, Mauffret A (1990) Iberian plate motions during the Mesozoic. Tectonophysics 184(4):260–278

Mathey B (1987) Les flyschs Crétacé supérieur des Pyrénées Basques. Tesis Doctoral, Mém. Univ. de Dijon 12:392

Mattauer M (1968) Les traits structuraux essentials de la chaîne pyrénéene. Rev Géogr Phys Géol Dyn 10:3–11

Mary C, Moreau MG, Orue-Etxebarría X, Apellaniz E, Courtillot V (1991) Biostratigraphy and magnetostratigraphy of the cretaceous/tertiary Sopelana section (Basque country). Earth Planet Sci Lett 106:133–150

McElhinny MW (1964) Statistical significance of the fold-test in paleomagnetism. Geophys J R Astron Soc 8:338–340

McFadden PL, Lowes FJ (1981) The fold test in paleomagnetism. Geophys J R Astron Soc 67:53–58

McFadden PL, McElhinny MW (1988) The combined analysis of remagnetisation circles and direct observations in paleomagnetism. Earth Planet Sci Lett 87:161–172

Montigny R, Azambre B, Rossy M, Thuizat R (1986) K–Ar study of Cretaceous magmatism and metamorphism in the Pyrenees: age and length of rotation of the Iberian peninsula. Tectonophysics 129:257–273

Moreau MG, Cojan J, Ory J (1994) Mechanisms of remanent magnetization acquisition in marl and limestone alterations; case study, Upper Cretaceous (Chron 31–30), Sopelana, Basque country. Earth Planet Sci Lett 123:15–37

Moreau MG, Berthou JY, Malod JA (1997) New paleomagnetic mesozoic data from the Algarve (Portugal): fast rotation of Iberia between Hauterivian and the Aptian. Earth Planet Sci Lett 146:689–671

Olivet JL (1996) La cinématique de la plaque Ibérique. Bull Cent Rech Explor Prod Elf Aquitaine 20:131–195

Osete ML, Osete C, Giallanella PR, Villalaín JJ (2000) Paleolatitudes de la Placa Ibérica durante el Jurásico. Programas y resúmenes, II. Asamblea Hispano-Portuguesa de Geodesia y Geofísica, pp 311–312

Palencia A (2005) Estudio paleomagnético de rocas de edad jurásica de la Península Ibérica y el sur de Marruecos. Ph.D. Thesis. Universidad Complutense de Madrid, p 275

Pedreira D, Pulgar JA, Gallart J, Díaz J (2003) Seismic evidence of Alpine crustal thickenning and wedging from the western Pyrenees to the Cantabrian Mountains (north Iberia). J Geophys Res 108(2204):10/1–10/21

Pujalte V, Baceta JI, Dinarès-Turell J, Orue-Etxebarría X, Parès JM, Payros A (1995) Biostratigraphic and magnetostratigraphic intercallibration of latest Cretaceous and Paleocene depositional sequences from the deep-water Basque Basin, western Pyrenees, Spain. Earth Planet Sci Lett 136(1–2):17–30

Ríos JM (1948) Diapirismo. Bol Geol Min España 60:153–390

Roest WR, Srivastava SP (1991) Kinematics of the plate boundaries between Eurasia, Iberia and Africa in the North Atlantic from late Cretaceous to the present. Geology 19:613–616

Roggenthen WM (1976) Magnetic stratigraphy of the Paleocene; a comparison between Spain and Italy. In: Pialli G (eds) Paleomagnetic stratigraphy of pelagic carbonate sediments, vol 15. Memorie della Societa Geologica Italiana, pp 73–82

Schott JJ, Peres A (1987) Paleomagnetism of Permo-Triassic redbeds from the Asturias and Cantabric chain (northern Spain): evidence for strong lower Tertiary remagnetizations. Tectonophysics 140:179–191

Schott JJ, Montigny R, Thuizat R (1981) Paleomagnetism and potassium-argon age of the Messejana Dyke (Portugal and Spain): angular limitation to the rotation of the Iberian Peninsula since the Middle Jurassic. Earth Planet Sci Lett 53:457–470

Shipunov SV (1997) Synfolding magnetization: detection, testing and geological applications. Geophys J Int 130:405–410

Srivastava SP, Roest WR, Kovacs LC, Oakey G, Lévesque S, Verhoef J, Macnab R (1990) Motion of Iberia since the late

Jurassic: results from detailed aeromagnetic measurements in the Newfoundland Basin. Tectonophysics 184(4):229–260
Stauffer KW, Tarling DH (1971) Age of the Bay of Biscay: new paleomagnetic evidence. L'histoire structurale de Golfe de Gascogne. Ed Technip, Paris
Steiner MB, Ogg JB, Meléndez G, Sequeiros L (1985) Jurassic magnetostratigraphy, 2. Middle-late Oxfordian of Aguilón, Iberian Cordillera, northern Spain. Earth Planet Sci Lett 76:151–166
Vandenberg J (1980) New paleomagnetic data from the Iberian Peninsula. Geol Mijnbouw 59(1):49–60
Van der Voo R (1993) Paleomagnetism of the Atlantic, Tethys and Iapetus Oceans. Cambridge University Press, Cambridge, pp 411
Waldhör M, Appel E (2006) Intersections of remanence small circles: new tools to improve data processing and interpretation in paleomagnetism. Geophys J Int 166:33–45